Characterisation of abrasive water-jet process for drilling titanium and carbon fibre reinforced polymer stacks

Gustavo A Escobar-Palafox [*], Krystian K Wika, Rosemary S Gault and Keith Ridgway

AMRC, University of Sheffield, Advanced Manufacturing Park, Wallis Way, Catcliffe, Rotherham, S60 5TZ, UK

*corresponding author: g.escobar@amrc.co.uk

Abstract. Experiments were carried out in stacks composed of titanium and carbon-fibre-reinforced polymer (CFRP) with the aim to investigate the effect of water-jet process variables on drilled diameter and surface condition. A design of experiments (DoE) approach was taken, considering variables such as water pressure, traverse rate, abrasive mass flow and stack set-up. Two different set-ups were investigated: CFRP over titanium (CFRP/Ti) and vice versa (Ti/CFRP). The experimental variables were related to taper ratio, surface roughness of the hole bore, hole quality and surface condition. Statistical analysis was carried out in order to develop mathematical models which include process variables interactions and quadratic terms. This led to models with high correlation and prediction power; which allow a better understanding of the process and can form the base for further process optimisation. The models were validated with additional experiments and showed good agreement with the water-jet system. The results showed that set-up and its interaction with other process variables has a strong influence on the performance of the abrasive water-jet system.

Keywords: Abrasive Waterjet Machining; CFRP Titanium Stacks

1. Introduction

Hybrid structures are increasingly being used in industries such as aerospace to further improve the strength-to-weight ratio of components. Composites are often stacked together with metals such as titanium or aluminium or with other composite materials [1]. These materials can be joined in many variations, such as composite over titanium as shown in Figure 1, vice versa and in multi-layer stacks. The total stack thickness may also vary with different thicknesses of individual plates.

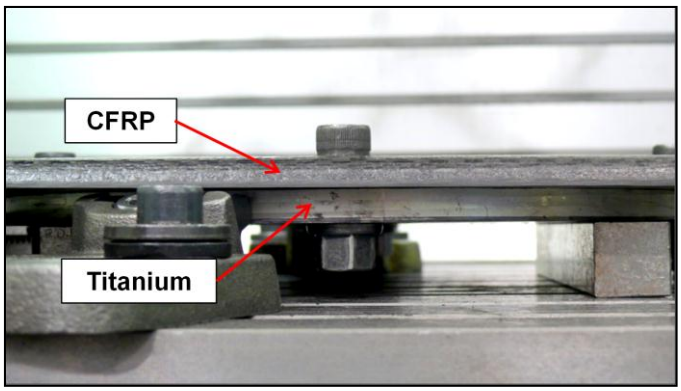

Figure 1 CFRP/Ti stack

As a joining method, holes are drilled through stacked materials and bolts are used to fix the plates together. The composite/titanium stack combination has the highest difficulty of drilling compared to the aforementioned structures, due to the risk of hole sidewalls erosion caused during the titanium chip evacuation [2]. Various manufacturing processes can be used to drill holes through the hybrid combination such as orbital drilling, ultrasonic assisted drilling, etc. A small improvement in the manufacturing process may translate into cost savings and higher production rates due to the high number of holes required when assembling components [3]. Moreover, the process has to meet specific requirements. Hole quality may be defined by hole diameter (cylindricity and lack of variation of diameter throughout the stacks), hole entry and exit damage, surface texture and surface integrity; for composite materials, delamination and roundness are the most important [4, 5].

The machining of hybrid structures has posed new challenges to conventional manufacturing chip-cutting processes. Titanium is known to be a difficult-to-machine material mainly due to its low thermal conductivity coefficient [6]. This causes the heat generated while cutting to concentrate on the tool tip, significantly decreasing the tool life [7]. On the other hand, the abrasive nature of composites makes this material hard to machine, affecting the quality of the hole and the tool life [8]. When the two materials are combined, the difficulties associated with drilling are further aggravated. In order to alleviate these problems, different tool geometries [9, 10], tool materials/substrates [11] and tool cooling methods [12] have been investigated. Alternative manufacturing process for drilling CFRP/Ti stacks such as abrasive water jetting (AWJ) have been less reported.

AWJ is a machining process where a compressed, high velocity, water stream carrying abrasive particles, impinges on the work-piece surface, removing the material by erosion. The AWJ process has some unique elements making this manufacturing method very competitive in comparison to other cutting processes, such as laser cutting or traditional drilling or milling. Abrasive waterjet cutting is very versatile being able to mill, drill, and turn or to create pockets and slots within just one machine. Furthermore, the lack of heat affected zone is advantageous, as there is no thermal distortion on cut surfaces [13, 14].

AWJ is capable of cutting a variety of materials such as glass, metals [15] and composites [8, 16, 17]. When machining composites, delamination has been recognised as one of the main types of damage, especially when slots and holes are being produced [18]. It has been demonstrated that the damage begins due to the shock wave impact of the water stream on the material and continues propagating as long as the water jet is applied [17]. The jet thrust force pushes uncut plies; which as a result of decreasing cutting thickness are weakened and can easily deform and delaminate.

Other features that are characteristic of surfaces produced by AWJ are due to the intrinsic characteristics of the kerf. The edges on the top of the work-piece are generally rounded due to plastic deformation and/or the abrasive nature of the water jet. The quality of the base of the work-piece is affected by exit burrs (typically for titanium plate) [13, 14]. AWJ may produce a taper surface where the top kerf is wider than the bottom; this taper angle can be minimised by reducing traverse speed and increasing the water pressure [19].

The objective of this study is to characterise the AWJ process for drilling through stacks composed of titanium and CFRP by relating water-jet process variables to hole quality and surface condition for different set-ups of stacks.

2. Methodology

Experiments were carried out with the aim of characterising the AWJ process for drilling holes in CFRP-Ti stacks. AWJ Critical Process Parameters (CPPs) were related to Critical Quality Attributes (CQA) relevant to drilling CFRP-Ti stacks. A Design of Experiments (DoE) approach was used in order to build mathematical models of these relationships. DoE is a useful statistical technique to identify important CPPs and their impact on the Critical CQAs [20].

The CPPs involved in AWJ have been classified as [21]:

- Cutting factors: stand-off distance, traverse direction, traverse rate, impact angle, number of passes;

- Hydraulic factors: water pressure, orifice diameter;
- Abrasive factors: abrasive feed rate, abrasive material, particle diameter, abrasive mass flow rate, abrasive size distribution, abrasive particle shape, abrasive hardness;
- Mixing factors: focus diameter, focus length, abrasive feed direction, material of focusing tube.

The DoE used in this study incorporates four water-jet CPPs: traverse rate, water pressure, abrasive feed rate and stack set-up (categorical variable). The stand-off distance, nozzle orifice diameter and abrasive grit size (garnet) were kept constant. The DoE consisted of a Rechtschaffner design, which is a saturated design of resolution V, in which main effects and two-factor interactions can be estimated if three-factor and higher order interactions are negligible [22]. In this way, an interaction model can be built. A centre point for each categorical variable was added to the design and repeated two times, in order to estimate the variability and repeatability of the system and detect any non-linearity in the system's responses. Table 1 provides a list of the DoE factors and their corresponding levels.

Table 1 CPPs and their corresponding levels

CPP, units (abbreviation)	Level	
	Low	High
Water pressure, nar (P)	2,760	4,140
Stand-off distance, mm (sd)	2	
Traverse rate, mm/min (Tr)	5	20
Abrasive mass flow, kg/min (m)	0.3	0.8
Abrasive grit (Abr)	80	
Nozzle/orifice diameter, mm (Noz)	0.25/0.76	
Stack set-up (Sup)	CFRP/Ti	Ti/CFRP

The experiments were carried out on a 3-axis ZX-513 WardJet AWJ system, equipped with a 50HP Accustream water pump. The experiments consisted of using the experimental parameters in Table 1 to drill 10 mm holes in two different stack set-ups - CFRP on Titanium and Titanium on CFRP. The test-piece was a 300mm diameter rolled, annealed Ti-6Al-4V disc with a thickness of 14 mm bolted onto a 300 x 300 x 13mm single stack of CFRP plate. The Titanium material had a reported yield stress of 990MPa, tensile strength of 1050MPa and 12% elongation. The CFRP material was a bidirectional composite plate with a single ply thickness of 0.25 mm and [0/90°] ply orientation made of CYCOM® 977-2 Toughened Epoxy Resin and Toho Tenax® High Strength HTA40 E13 6K 400tex fibre type. The plate with quasi-isotropic layout was cured in the autoclave at 90 psi pressure, at 175°C for 90 minutes. Figure 2 shows a picture of the experimental set up on the AWJ machine table.

Figure 2 Experimental set-up for the Ti over CFRP configuration

Measurements of average surface roughness, Ra, were taken in the bore of the hole using a Mitutoyo SJ-301 surface tester. The measurements were taken along the axial direction of the bore with a scanning length of 5.6mm and cut-off distance of 0.5mm. Four repeated measurements were taken. The mathematical mean was used for the statistical analysis.

The diameter and cylindricity of the holes were measured using a Metris Coordinate Measuring Machine (CMM) with a scanning probe equipped with a 3mm ruby. Measurements were taken at two different depth levels of the Titanium test-piece (spaced 13 mm) and two levels of the CFRP (spaced 9 mm); in this way, the reduction in diameter (taper ratio) can be calculated. The mathematical mean of the ratio between the diameters was used for the statistical analysis.

Two Titanium sample cut-ups were produced with the aim of investigating the effect of set-up on microstructural features. The cut-up samples were produced with parameters used for the centre point (i.e P = 3,447 bar, Tr = 12.5 mm/min, m = 0.55 kg/min) for the two different set-ups. The cut ups were hot-mounted in Bakelite, ground with SiC paper, polished with diamond grit and finished with 0.5 μm colloidal silica. Measurements of maximum level of depth observed in regards to the impact of the abrasive material were taken.

3. Results and analysis

The analysis was carried out using MODDE 9.1 software using the Partial Least Squares (PLS) method. Theoretical and actual design plans were identical. A total of 15 experiments (including the 2 centre points for each categorical variable) were carried out for the analysis. Additionally, two experiments were carried out for model validation.

3.1 Surface roughness

The titanium samples presented a wide range of mean average surface roughness; the measurements were within the range of 1.31 to 2.33 μm. Figure 3 displays a plot of replications for the titanium surface roughness measurements. The centre points had fairly good repeatability and were located roughly in the centre of the measurement range. The mean surface roughness of the titanium over CFRP set-up (index 12 and 13) had a lower mean surface roughness than the CFRP/Titanium set-up (index 14 and 15). The experiments with low traverse rate, high abrasive mass rate and Ti/CFRP set-up (index 3 and 11) disregarding the water pressure had the lowest mean surface roughness.

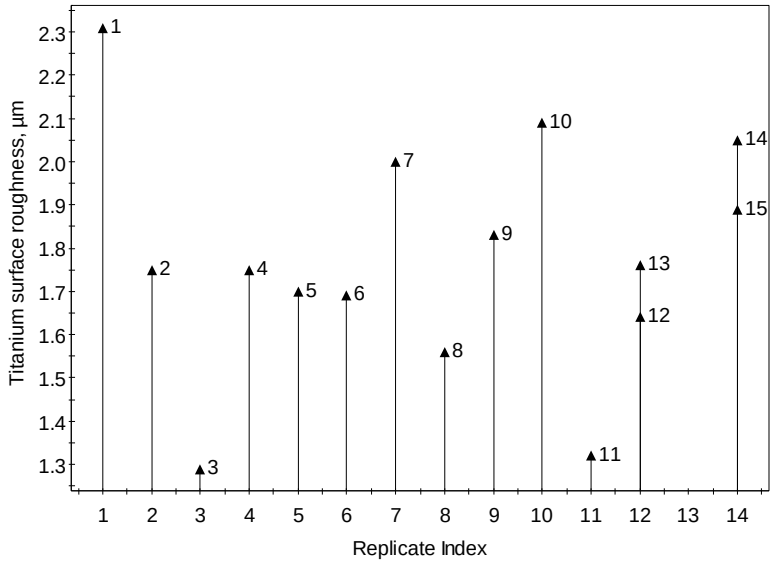

Figure 3 Titanium mean average surface roughness plot of replications

The mean average surface roughness measurements of the CFRP samples had a wider range; presenting a minimum mean surface roughness measurement of 2.7 and a maximum of 7.04 µm. The centre points had fairly good repeatability and were located at the lower end of the range. The roughest surface (index 8) belonged to the experiment with high pressure, low traverse rate, low mass rate and Ti/CFRP set-up.

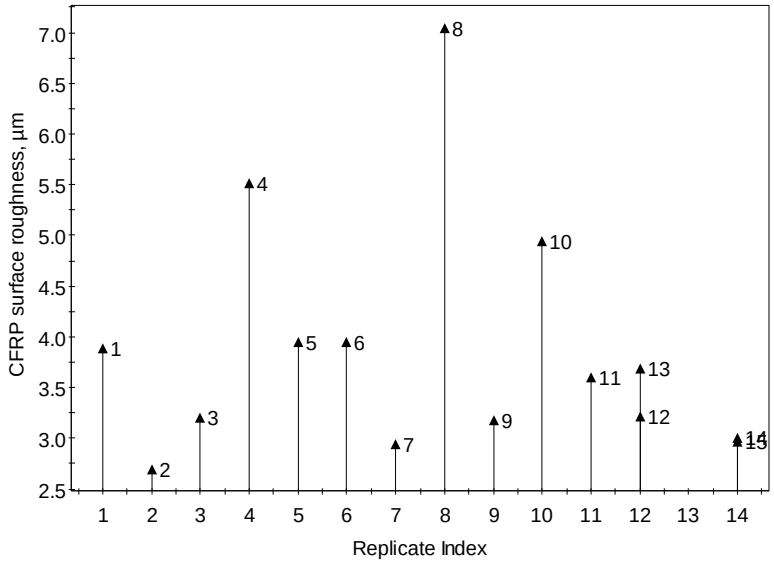

Figure 4 CFRP mean average surface roughness plot of replications

The titanium mean surface roughness data presented a bell shaped normal distribution which allowed the statistical analysis of the raw data. The experimental design had a good performance as measured by the condition number (2.15). The regression coefficients for the Titanium surface roughness model are shown in Figure 5. The CPP that had the strongest influence in the mean surface roughness of the bore of the hole of the titanium samples was the set-up. Mean surface roughness of the bore of the

titanium hole reduces with the Ti/CFRP set up. The abrasive particles have a higher force and impact angle, creating a smoother surface; whereas for the CFRP/Ti set-up the particles have lost force and impact at shallower angles as they first penetrate the CFRP material. Water pressure and abrasive mass flow had a strong effect on the mean surface roughness; this decreases with increasing pressure and abrasive mass flow. Traverse speed did not have an influence on surface roughness within the range of 5 to 20mm/min. The interaction between pressure and abrasive mass flow was significant. Abrasive mass rate has a stronger effect on the mean surface roughness of the bore of the titanium hole for lower pressures than for higher ones. This may be attributed to the abrasive particles penetrating more the material at higher pressures whereas for lower pressures an increase in abrasive particles compensates for this. The mathematical model for relating the mean surface roughness of the bore of the hole of titanium had a good fit as expressed by the R^2 statistic (0.971) and excellent prediction power as indicated by Q^2 (0.867).

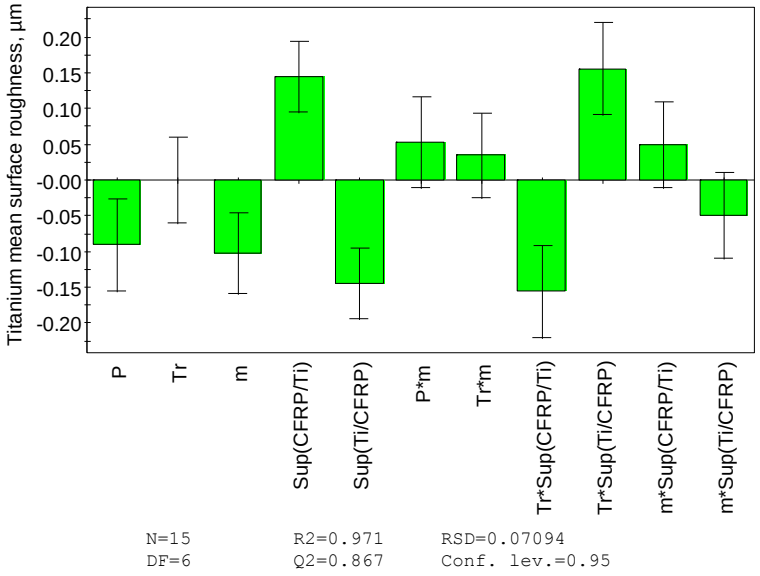

Figure 5 Regression coefficients for titanium mean average surface roughness

The CFRP mean average surface roughness data had to be pre-processed by applying a logarithmic transformation (10Log(y)). The experiment design had a very good performance with a condition number of 1.85. The regression coefficients for the CFRP mean surface roughness of the bore are shown in Figure 6. The main CPP affecting mean surface roughness was abrasive mass flow rate; increasing the flow of abrasive reduced the surface roughness; as this allows more particles to impinge on the surface. The interaction between abrasive mass flow and set-up was significant; the effect of abrasive mass rate depends on the set-up. The abrasive rate has a stronger effect for the Ti/CFRP set-up; more particles seem to be needed to penetrate through the CFRP and reach the titanium material. The interaction between set-up and traverse rate was also strong. For the Ti/CFRP set-up, increasing the traverse rate decreases the mean surface roughness of the CFRP. In contrast, for the CFRP/Ti set up, increasing the surface roughness increases the mean surface roughness. Smoother CFRP surfaces were achieved for the CFRP-Ti set-up.

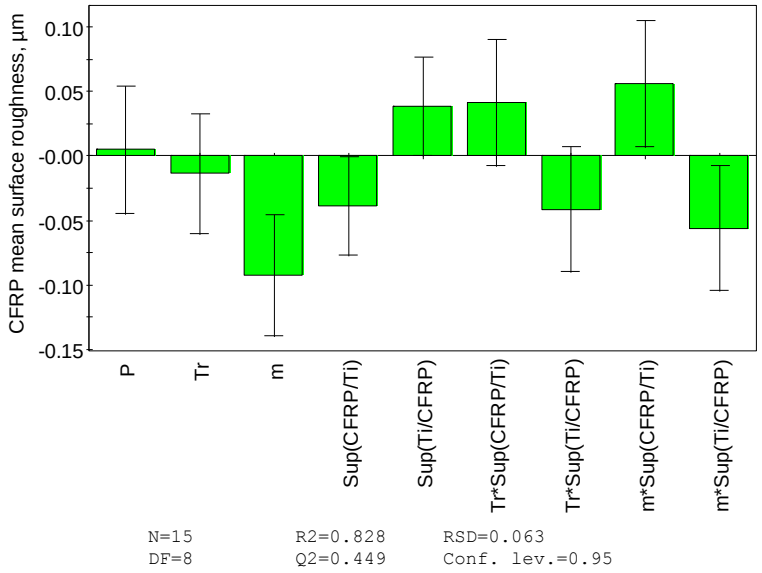

Figure 6 Regression coefficients for CFRP mean average surface roughness

With the mathematical model produced, response plots showing the relationship between CPPs can be plotted. Figure 7 displays a contour plot of Ti mean surface roughness related to water pressure and abrasive mass flow for the Ti/CFRP set-up. A slight non-linearity of the system can be noticed; which is due to the interaction between abrasive mass flow and water pressure. Surface roughness can be reduced by increasing the water pressure and/or increasing the abrasive mass flow.

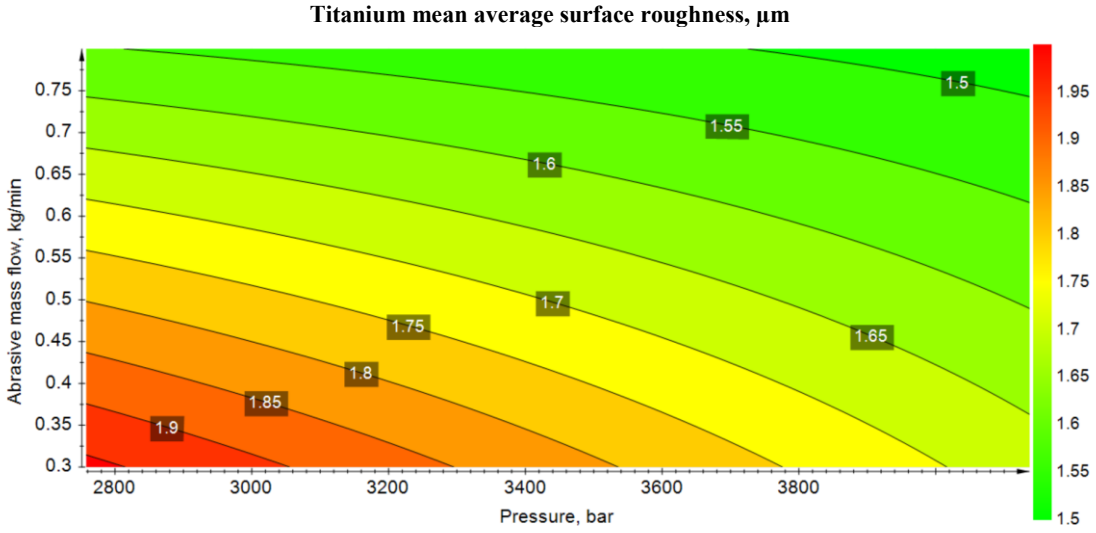

Figure 7 Ti mean surface roughness contour plot
Tr = 12.5 mm/min; Set-up = Ti/CFRP

A contour plot for CFRP mean surface roughness is shown in Figure 8; this plot relates traverse rate to abrasive mass flow for the CFRP/Ti set-up. The plot presents a linear behaviour as no interactions are related to abrasive mass flow and traverse rate. The mean average surface roughness of CFRP can be minimised by increasing the abrasive mass flow and reducing traverse rate, for the CFRP/Ti set-up. However, for the Ti/CFRP set-up, increasing the traverse rate decreases mean average surface roughness of CFRP; as shown in Figure 9.

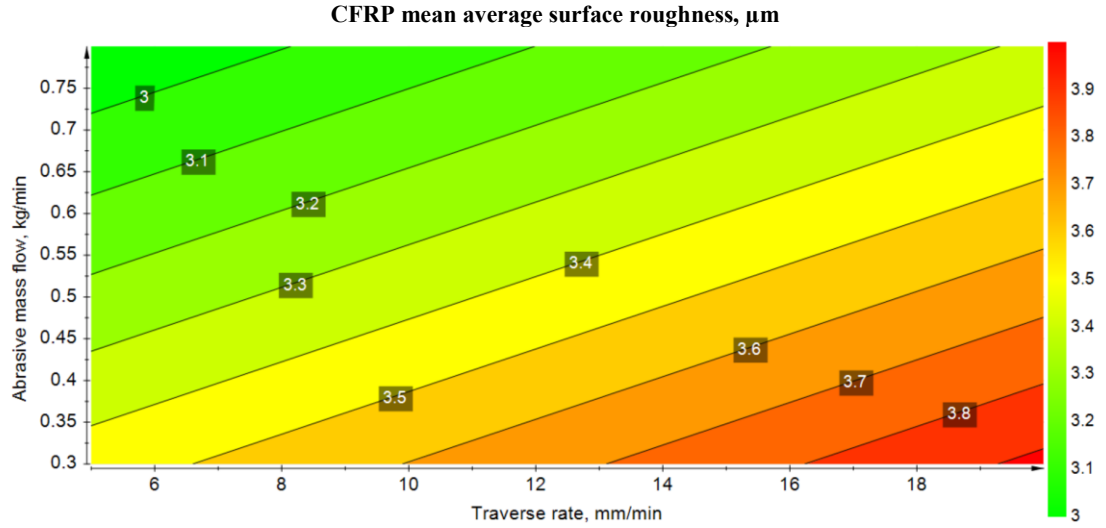

Figure 8 CFRP mean surface roughness contour plot
P = 3,447 bar; Set-up = CFRP/Ti

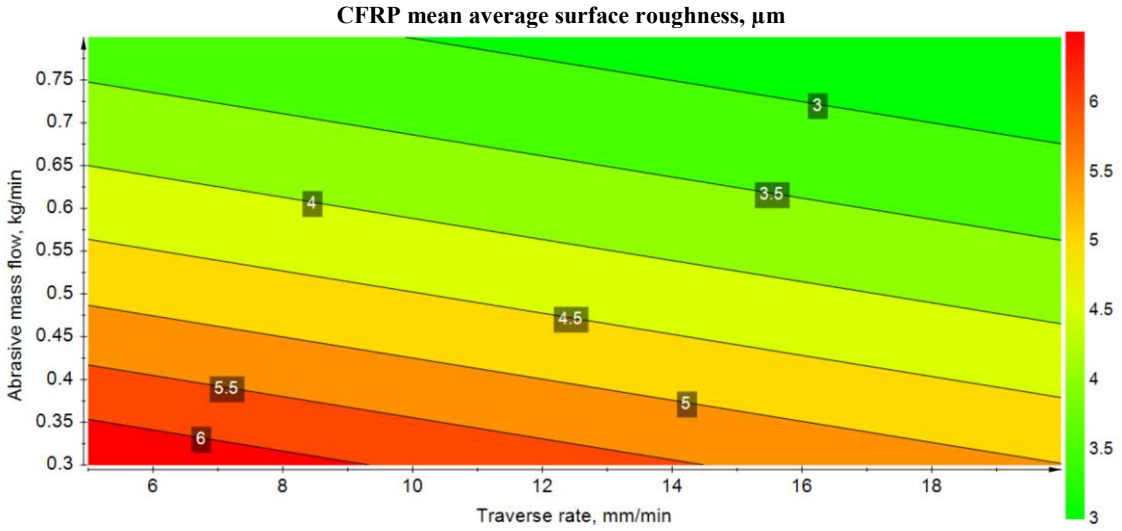

Figure 9 CFRP mean surface roughness contour plot
P = 3,447 bar; Set-up = Ti/CFRP

3.2 Taper ratio

All titanium samples presented a taper ratio less than 1, regardless the experimental parameters. The maximum and minimum taper ratios were 0.9956 and 0.9484 respectively. The experimental runs that had a lower taper ratio (replicate index 3 and 8) were the ones produced with high pressure, low traverse rate and Ti/CFRP set-up, irrespectively of the abrasive mass flow. Contrary to this, the experiments that had a higher taper ratio (replicate index 2 and 10) were the ones produced with low water pressure, high traverse rate and Ti/CFRP set-up. The centre points (index 12/14 and 14/15) had good repeatability. The centre points belonging to the Ti/CFRP set-up had a higher taper ratio.

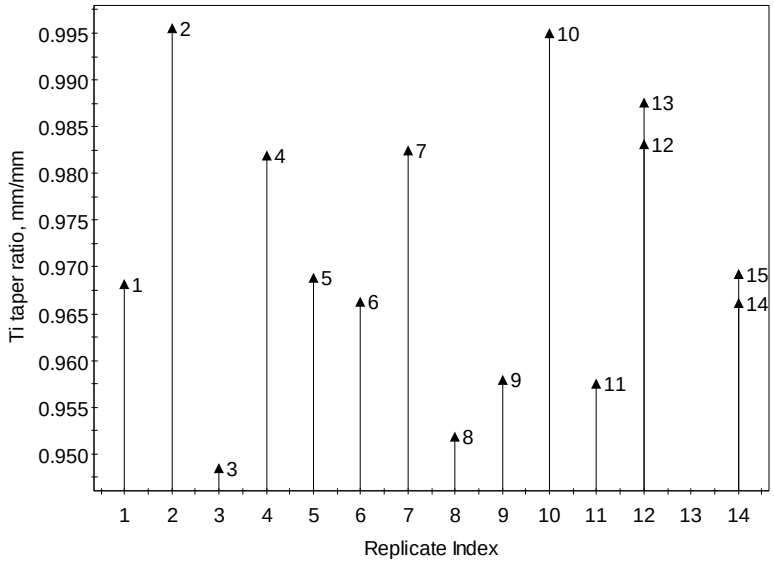

Figure 10 Titanium taper ratio plot of replications

The measurements of mean CFRP taper ratio were divided into two distinctive blocks as shown in Figure 11. The experiments conducted with the Ti/CFRP set-up had a CFRP taper ratio less than one whereas the ones carried out with the CFRP/Ti set-up had a taper ratio greater than one. The replicates had fairly good repeatability.

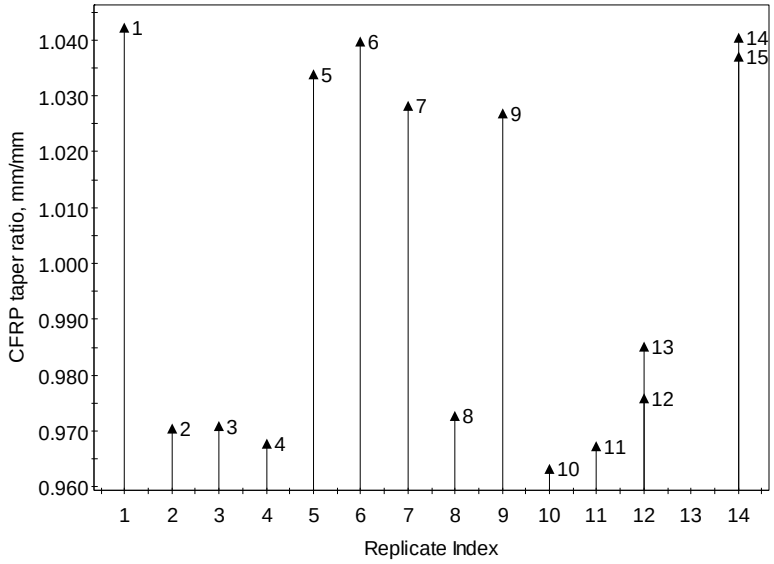

Figure 11 CFRP taper ratio plot of replications

The mathematical model for the titanium taper ratio is presented in Figure 12 as regression coefficients. The experiment design had a good performance with a condition number of 1.852. The CPP that had the strongest influence on the mean taper ratio of titanium was the interaction between traverse rate and set-up. For the Ti/CFRP set-up, lowering the traverse rate increases the taper ratio while for the CFRP/Ti lowering the traverse rate decreases the taper ratio. The interaction between pressure and set-up was also significant. For the Ti/CFRP setting lowering the pressure has the effect of increasing the taper ratio; whereas for the CFRP/Ti set-up the taper ratio increases with increasing

water pressure; as the water jet has more power to penetrate through the titanium producing a straighter cut. The Ti taper ratio model had a good fit (R^2 = 0.897) and very good prediction power (Q^2 = 0.713).

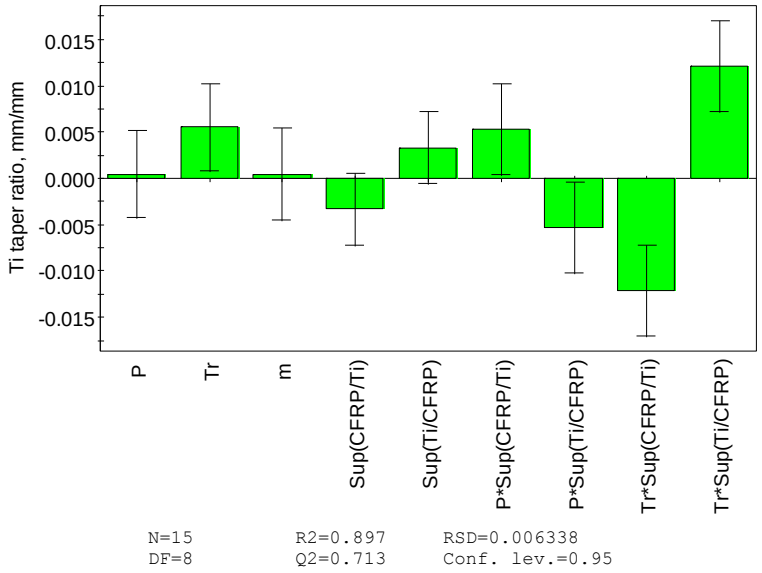

Figure 12 Regression coefficients for titanium mean taper ratio

The regression coefficients for the CFRP taper ratio model are shown in Figure 13. The model had a fairly good performance as indicated by the condition number (3.72). The factor that dominates the model is the set-up. Higher CFRP mean taper ratios were achieved with the CFRP/Ti set-up; as the water jet cuts the CFRP material first with high force. Water pressure and its quadratic term had an effect on taper ratio; increasing water pressure to a certain degree (~3,500 bar) increases taper ratio; after this further increases reduces the CFRP taper ratio.

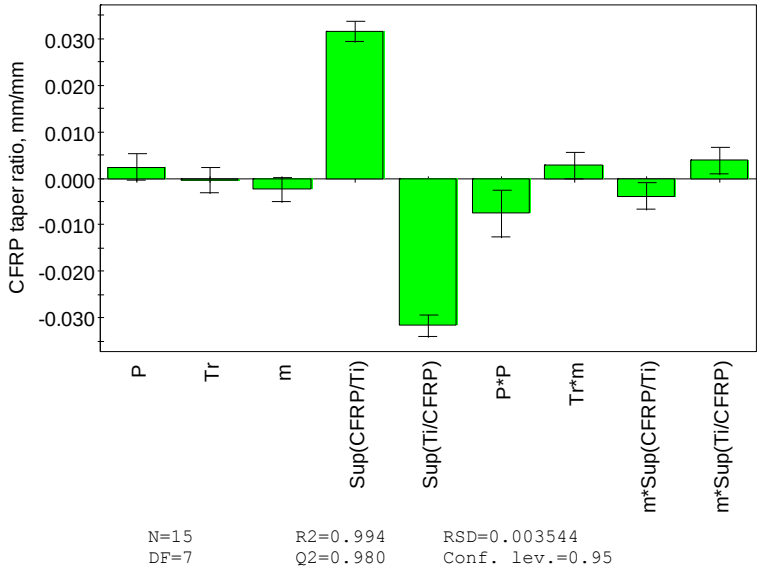

Figure 13 Regression coefficients for CFRP mean taper ratio

A contour plot relating traverse rate and water pressure to mean taper ratio of CFRP is displayed in Figure 14. The figure shows the non-linear behaviour of the water jet system. Similar levels of taper

ratio can be achieved at both, low and higher pressure. Taper ratio closer to 1 can be achieved either at lower or higher pressure with low traverse rate.

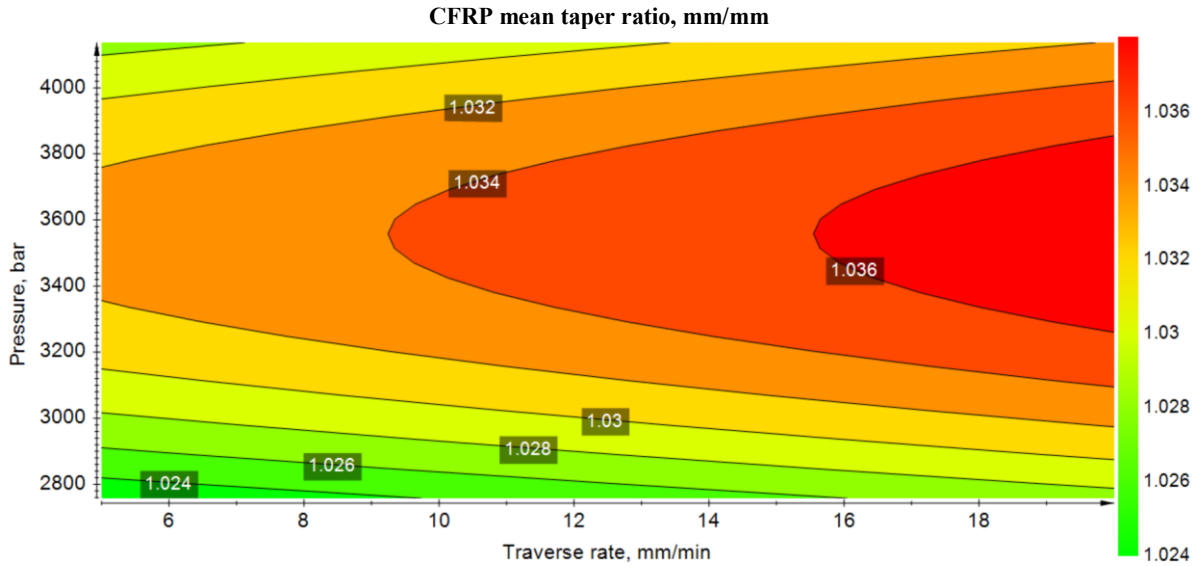

Figure 14 CFRP mean taper ratio contour plot
m = 0.80 kg/min; Set-up = CFRP/Ti

3.3 Microstructural features

Two samples belonging to the centre points (P = 3447 bar; Tr = 12.5 mm/min; m = 0.55 Ti/CFRP and CFRP/Ti) were examined and shown in Figure 15 and Figure 16. Both samples contained a certain level of deformation (less than 25 µm). The CFRP/Ti sample presented a surface with deeper craters, better explained by the higher surface roughness (7.05 compared to 3.7µm). The samples indicated a material removal mechanism by micro-cutting and crack propagation; with some evident surface cracks. However, no sub-surface deformation or cracking in the sub-surface was noted.

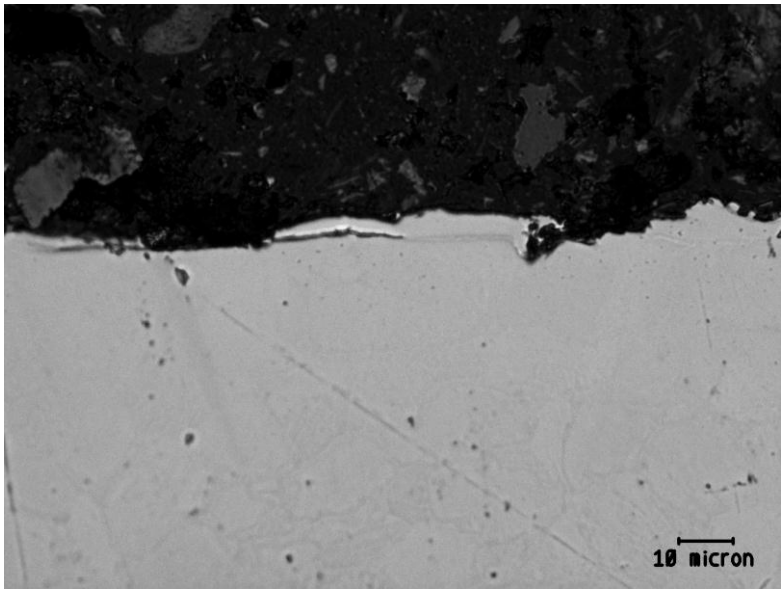

Figure 15 Micrograph of titanium sample
(P=3447bar; Tr=12.5mm/min; m=0.55; Ti/CFRP)

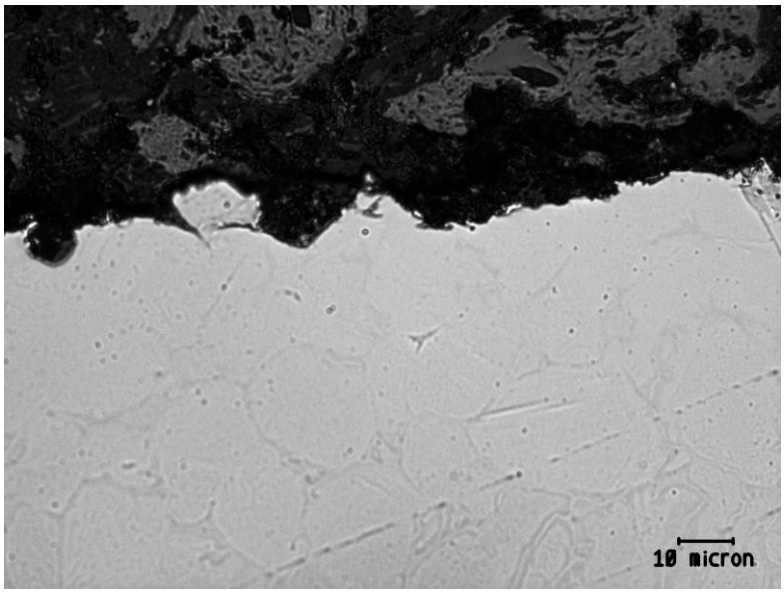

Figure 16 Micrograph of titanium sample
(P=3447bar; Tr=12.5mm/min; m=0.55; CFRP/Ti)

3.4 Model validation

The four models produced, Ti mean average surface roughness, CFRP mean average surface roughness, Ti taper ratio and CFRP taper ratio were validated with two additional experiments. The experiments fell within the range of experimental parameters and corresponded to the two different settings: P = 2758 bar; Tr = 10 mm/min; m = 0.64 kg/min; Ti/CFRP and CFRP/Ti. The Ti mean surface roughness model predicted 2.05 μm for the CFRP/Ti set-up and 1.63 μm for the Ti/CFRP set up; actual measurements were 2.06 and 1.78 μm respectively. This results in a 0.49% error for the Ti model and 8.4% error for the CFRP model. The Ti taper ratio model predicted a taper ratio of 0.096502 and 0.974371 when actual values were 0.96504 and 0.981728 (less than 1% error). The CFRP taper ratio model predicted a mean taper ratio of 1.02868 and 0.968413 and actual values were 1.04337 and 0.977423; which error was less than 2%.

4. Conclusions and further research

The process of drilling holes through CFRP/Ti stacks by AWJ was characterised; using statistical analysis water-jet CPPs were related CQAs. Four mathematical models were built which link water pressure, traverse rate, abrasive mass flow and set-up (CFRP/Ti or Ti/CFRP) to mean average surface roughness of the titanium bore, mean average surface roughness of the CFRP hole, taper ratio of the titanium hole and taper ratio of the CFRP hole. Additionally, microstructural features in the titanium hole were investigated. The models presented good fit, high prediction power and had good agreement with the water-jet system.

The influence of the main four CPPs and interactions on CQAs is summarised in Table 2; the CPP with the strongest effect is marked with an asterisk (*); the direction of change is indicated with an arrow. Mean average surface roughness of the two materials reduces with increasing abrasive mass flow. Setting up the material at the top reduced this material's mean average surface roughness. Traverse rate did not have a strong influence in surface roughness but rather its interaction with the set up. When titanium is positioned at the top, lower traverse rate minimises the Ra in Ti whereas higher traverse rates minimises the Ra in CFRP. However, when CFRP is on the top higher traverse rates

minimises the Ra in Ti and low traverse rate minimise the Ra on CFRP. The set-up has a strong effect on taper ratio of both the titanium and CFRP material. For titanium, the interaction between the set-up traverse rate and pressure are important whereas for the CFRP the interaction with the abrasive mass flow rate is significant.

Table 2 Summary of influence of CPPs on CQAs

CQA/CPP	P	Tr	m	Sup	Tr·Sup	m·Sup	P·Sup	Tr·m	P·P
Ti Ra	↑		↑	Ti/CFRP	✓*				
CFRP Ra			↑*	CFRP/Ti	✓	✓			
Ti Taper		↑		Ti/CFRP	✓*		✓		
CFRP Taper				CFRP/Ti*		✓		✓	✓

Analysis of the microstructure of titanium revealed some craters due to the micro-cutting mechanism; no cracks in the sub-surface were noticed.

As a follow-up investigation CPPs that were not considered in the design such as stand-off distance, abrasive type, abrasive size, nozzle orifice combination, etc. can be incorporated in the model. Furthermore, system optimisation is needed.

Acknowledgement

The authors acknowledge the support of the European Commission through the 7th Framework Programme, Factory of the Future Theme, Project number 283336 - REFORM.

5. References

1. Massarweh, W.A. and C.L.J. Hough, *Performance analysis for drilling in thermoplastic composite-aluminum stacks.* Composite Material Technology, 1992. **45**: p. 253-259.
2. Kolesnikov, B., L. Herbeck, and A. Fink, *CFRP/titanium hybrid material for improving composite bolted joints.* Composite Structures, 2008. **83**: p. 368-380.
3. Branson, T.H., *Drilling of graphite/bismaleimide and titanium stacks*, 1999, University of Washington. p. 428.
4. Kim, D., M. Ramulu, and W. Pedersen, *Machinability of titanium/graphite hybrid composites in drilling.* Transactions of the North American Manufacturing Research Institution of SME, 2005. **33**: p. 445-452.
5. Roudge, M., et al., *Multi-layer Materials. Qualitative Approach of the Process.* International Journal of Materials and Forming, 2008. **1**(1): p. 949-952.
6. Ezugwu, E.O. and Z.M. Wang, *Titanium alloys and their machinability -a review.* Journal of Materials Processing Technology, 1997. **68**: p. 262-274.
7. Hartung, P.D. and B.M. Kramer, *Tool Wear in Machining Titanium.* Ann. CIRP, 1982. **31**(1): p. 75-80.
8. Wang, J., *Abrasive Waterjet Machining of Polymer Matrix Composites -Cutting Performance, Erosive Process and Predictive Models.* International Journal of Advanced Manufacturing Technology, 1999. **15**: p. 757-768.
9. Bhattacharyya, D. and H. D.P.W, *A study of hole drilling in kevlar composites.* Composites Science and Technology, 1998. **58**(2): p. 267-283.
10. Wika, K., et al., *Impact of Number of Flutes and Helix Angle on Tool Performance and Hole Quality in Drilling Composite/Titanium Stacks.* SAE Technical Paper 2011-01-2744, 2011. doi:10.4271/2011-01-2744.

11. Garrick, R., *Drilling Advanced Aircraft Structures with PCD (Poly-Crystalline Diamond) Drills.* SAE Technical Paper 2007-01-3893, 2007. doi:10.4271/2007-01-3893.
12. Yildiz, Y. and M. Nalbant, *A review of cryogenic cooling in machining processes.* Machine Tools and Manufacture, 2008. **48**: p. 947-964.
13. Momber, A.W. and R. Kovacevic, *Principles of Abrasive Water Jet Machining*1998, London: Springer Verlag Ltd.
14. Wang, J., *Abrasive Waterjet Machining of Engineering Materials* Materials Science Foundations. Vol. 19. 2003, Switzerland: Trans Tech Publications. 104.
15. Kong, M. and D.A. Axinte, *Capability of Advanced Abrasive Waterjet Machining and its Applications.* Applied Mechanics and Materials, 2011. **110-116**: p. 1674-1682.
16. Wang, J. and D.M. Guo, *A predictive depth of penetration model for abrasive waterjet cutting of polymer matrix composites.* Journal of Materials Processing Technology, 2002. **121**(2-3): p. 390-394.
17. Shanmugam, D.K., T. Nguyen, and J. Wang, *A study of delamination on graphite/epoxy composites in abrasive waterjet machining.* Composites Part A Applied Science and Manufacturing, 2008. **39**(6): p. 923-929.
18. Mazumdar, S., *Composites Manufacturing: Materials, Product, and Process Engineering*2001: CRC Press.
19. Shanmugam, D.K. and S.H. Masood, *An investigation on kerf characteristics in abrasive waterjet cutting of layered composites.* Journal of Materials Processing Technology, 2009. **209**(8): p. 3887-3893.
20. Eriksson, L., et al., *Design of Experiments, Principles and Applications*2008: Umetrics Academy.
21. Hloch, A., *Analysis of abrasive water jet factors influencing the cast aluminum surface roughness.* International Journal of Advanced Manufacturing Technology 2007. **1**(1): p. 1-10.
22. Qu, X.G., *Statistical properties of Rechschaffner designs.* Journal of Statistical Planning and Inference, 2007. **137**(7): p. 2156-2164.